

The Profitis Ilias deposit, Milos island, Greece: a case study of boiling in an epithermal system recorded by stable isotope and fluid inclusion data

J. Naden,

British Geological Survey, Keyworth, Notts, UK.

S. Kilias

National University of Athens, Department of Geology, Athens, Greece.

M.J. Leng

British Geological Survey (NERC Isotope Geosciences Laboratory), Keyworth, Notts, UK.

I. Cheliotis

Institute of Geology and Mineral Exploration, Athens, Greece.

T.J. Shepherd

British Geological Survey, Keyworth, Notts, UK.

B. Spiro

British Geological Survey (NERC Isotope Geosciences Laboratory), Keyworth, Notts, UK

ABSTRACT: Stable isotope (δD and $\delta^{18}\text{O}$) and microthermometric data are presented for the Profitis Ilias adularia-sericite-type epithermal gold deposit on Milos Island, Greece. The deposit was discovered by Midas Enterprise SA, and estimated reserves are 5 million tonnes grading at 4.4 g/t Au and 43 ppm Ag. Microthermometric data show that the system boiled. Stable isotope ratios were determined on inclusion-fluids (δD and $\delta^{18}\text{O}$) and vein quartz ($\delta^{18}\text{O}$). The inclusion-fluid data show fractionation trends consistent with single-stage steam separation and are broadly comparable to the currently active Milos geothermal system. The trends and comparisons in the fluid-mineral data are more difficult to interpret. This suggests that data derived by analysing both δD and $\delta^{18}\text{O}$ on inclusion-fluids can provide a better framework for interpreting fluid processes in epithermal systems than current methodologies based on calculating $\delta^{18}\text{O}$ from fluid-quartz equilibria.

1 INTRODUCTION

Stable isotope analyses (δD and $\delta^{18}\text{O}$) of inclusion fluids in quartz provide valuable insights into fluid sources, hydrothermal processes and fluid-rock interaction in a wide range of geological environments. Current methodologies for determining D/H and $^{18}\text{O}/^{16}\text{O}$, focus on measuring δD on extracted inclusion fluids and calculating $\delta^{18}\text{O}$ of the fluid by analysing the host quartz. Recently, procedures that analyse both δD and $\delta^{18}\text{O}$ on inclusion fluids have been developed for quartz and carbonates (e.g. Ohba, & Matsuo, 1988, Lécuyer & O'Neil, 1994). However, scientific opinions as to which approach is the most appropriate are divided (Vityk et al. 1993, Ohba et al. 1995). The indirect approach is not ideal, it relies on accurate determination of quartz precipitation temperatures, usually ascertained through fluid inclusion microthermometry. There is also the factor that there is evidence for isotopic dis-

equilibrium between quartz and the fluid phase at low temperatures (<250 °C) (e.g. Ligang et al. 1989). On the other hand, direct measurements also have problems in data interpretation. These centre on the fact that isotopic re-equilibration can occur after trapping and during cooling of the fluid inclusions (Ohba et al. 1995).

In this study, we present directly and indirectly measured δD and $\delta^{18}\text{O}$ data for adularia-sericite epithermal-Au mineralisation at Profitis Ilias on Milos Island (Aegean sea). A deposit closely linked to a modern geothermal reservoir, and whose geology, mineralogy and fluids inclusions are well characterised (Kilias et al. in press). In addition, the modern system is well documented mineralogically, geochemically and isotopically (e.g. Liakopoulos et al. 1991, Pflumio et al. 1991, Christianis & St. Seymour, 1995) and provides an excellent analogue for the epithermal-Au mineralisation.

2 GENERAL GEOLOGY

Milos Island is located at the western end of the Pleistocene-Pliocene Aegean Volcanic Arc. The island is still geothermally active and a high-enthalpy geothermal resource is located towards its centre. Geologically, the island comprises mainly calc-alkaline volcanic rocks (tuffs, pumice flows, ignimbrites, pyroclastic flows, domes and lava flows of andesitic-dacitic, and rhyolitic composition). The volcanic sequence is built on Miocene-Pliocene clastic and carbonate platform sediments, which unconformably overly Mesozoic(?) metamorphic basement rocks. Metalliferous mineralisation is predominantly located on the western end of the island in the oldest volcanic rocks. Two main styles are evident: stratiform Mn–Ba, and epithermal Ag–Au–Pb–Zn–Cu mineralisation.

The Profitis Ilias gold deposit is located in this zone, and is approximately 20km west of the active geothermal system. It was discovered by Midas Enterprise S.A, and is classified as an adularia–sericite type epithermal deposit. Estimated reserves are 5 million tonnes grading at 4.4 g/t Au and 43 ppm Ag and recently bonanza grades have been discovered in the vicinity. The deposit is closely associated with a horst and graben structure and is characterised by a series of interconnected veins that are commonly composite and crustiform-banded. Vein widths are up to 3 m and extend to depths of at least 300 m (relative to the present day surface).

3 MINERALISATION

Mineralisation is hosted in sericitised and argillised rhyolitic lapilli–tuffs and ignimbrites, and consists of pyrite, galena, chalcopryrite, native gold, and electrum. On the microscopic scale, minor adularia veinlets were also observed in the host rocks adjacent to the mineralisation. Three broad paragenetic stages of the mineralisation are recognised: 1. early, pre–ore mineralisation consists of barren microcrystalline quartz and pyrite; 2. main ore–stage mineralisation is characterised by deposition of coarse– and fine–grained sphalerite, galena, chalcopryrite, pyrite, and quartz. Free gold, in this association (1–50 μm in size; typically 1–10 μm), usually occupies interstices between, or is intergrown with, fine–grained quartz crystals, or coexists with oxidised sulphides; 3. post–ore mineralisation comprises barite intergrown with fine–grained quartz, and minor sulphides.

4 FLUID INCLUSIONS

Fluid inclusion data were obtained on drill–core samples and surface exposures of the veins. Two

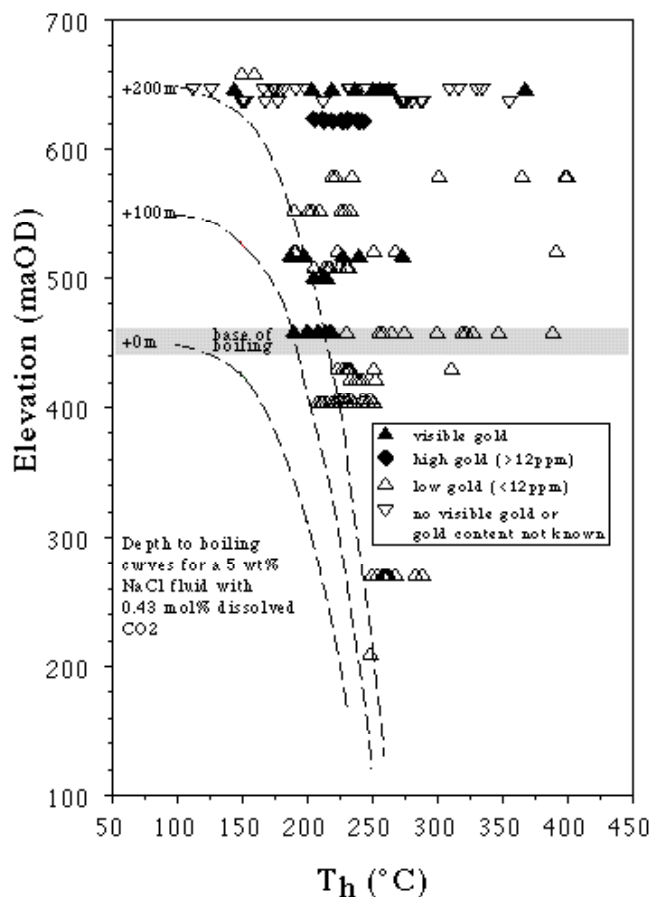


Figure 1. Depth– T_h relationships for the Milos ore stage fluids. Note that below 450m fluid inclusion homogenisation temperatures are tightly clustered, whilst above this level they exhibit a high degree of scatter. This is interpreted to represent heterogeneous trapping of fluid inclusions in a boiling epithermal system, with the base of boiling located at the 450m level (after Kilias et al. in press).

main inclusion types were identified: aqueous liquid– and vapour–rich. They occur in ore and post–ore quartz, sphalerite, and barite. Quartz and sphalerite contain predominantly liquid–rich primary inclusions, whereas barite contains relatively more (20% by number) vapour–rich inclusions in comparison.

Primary liquid–rich inclusions homogenise at temperatures between 112 and 399 $^{\circ}\text{C}$. The homogenisation temperature range for each stage is as follows: ore–stage: 145 to 399 $^{\circ}\text{C}$ (median 230 $^{\circ}\text{C}$); post–ore stage: 112 to 263 $^{\circ}\text{C}$ (median 175 $^{\circ}\text{C}$). Estimates of eutectic melting (–25 to –38 $^{\circ}\text{C}$) indicate the presence of divalent cations in the ore fluids, probably magnesium or calcium. Salinities of liquid–rich inclusions, based on microthermometric data, range between 0.1 and 11.4 wt% NaCl equiv. in ore–stage quartz and sphalerite, and between 0.93 and 8.5 wt% NaCl equiv. in post–ore barite. Vapour–rich inclusions in ore–stage quartz homogenise between 368 and 399 $^{\circ}\text{C}$, whilst vapour–rich inclusions in barite generally decrepitated before anticipated homogenisation.

Evidence for boiling, in the fluid inclusion data, is shown by examining the relationship between sam-

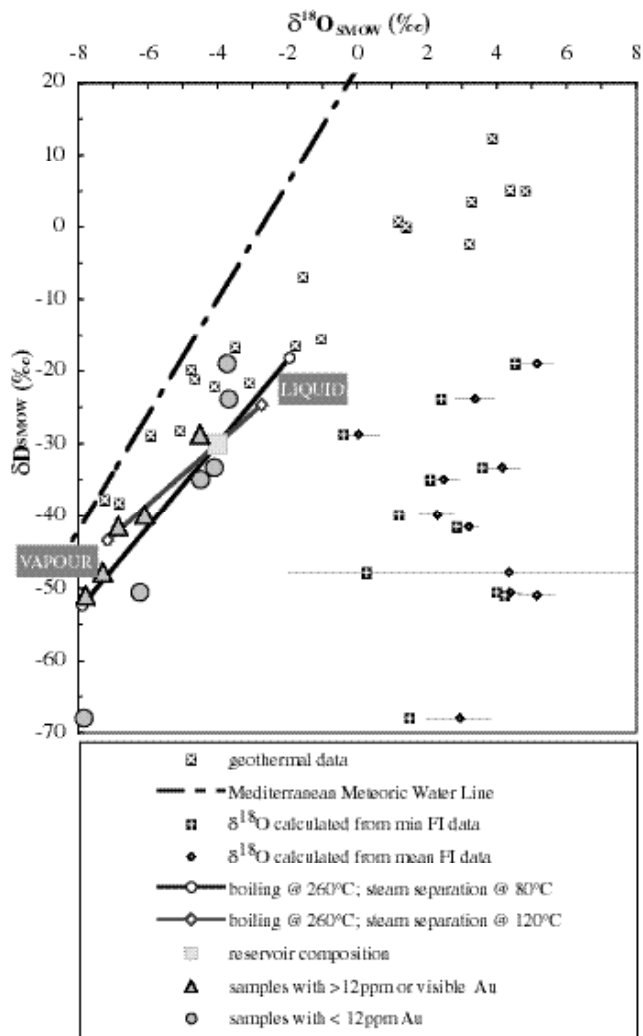


Figure 2. δD — $\delta^{18}O$ plot of Profitis Ilias inclusion fluids comparing uncorrected inclusion fluid data with calculated δD — $\delta^{18}O$ and stable isotope data for the modern geothermal system (data from Liakopoulos et al. 1991). For comparison, steam fractionation trends are also shown.

ple elevation and homogenisation temperature (Fig. 1). Two distinct distributions are evident. Below 450m fluid inclusion homogenisation temperatures are tightly clustered and vary only by 20 to 50°C. However, above this level homogenisation temperatures show extreme variation (sometimes over 150°C). This is attributed to the heterogeneous trapping of a boiling hydrothermal fluid in the upper levels of the system. The transition between the two distributions at 450m is interpreted as the base of boiling. Moreover, samples containing high gold values (>12ppm) or visible gold are exclusively located above this level.

STABLE ISOTOPE ANALYSES

To constrain further the role of boiling, quartz samples were selected for stable isotope analysis on the inclusion fluids. Combined δD and $\delta^{18}O$ were analysed on extracted fluid inclusion waters by CO_2 micro-equilibration methods to obtain both δD and $\delta^{18}O$ on the inclusion fluids. In addition, $\delta^{18}O$ was

measured, utilising the same samples, on the host quartz using standard fluorination techniques.

4.1 Oxygen isotopes

Oxygen isotope data for extracted inclusion fluids and quartz along with summary fluid inclusion and assay–elevation data are presented in Table 1. The data show a correlation between sample–elevation and $\delta^{18}O$ in both inclusion waters and quartz (Tab. 1). With the exception of the sample from the highest elevation (657 m, sample G2185), which has a $\delta^{18}O_{\text{water}}$ of -4.5‰ , $\delta^{18}O$ of inclusion waters steadily decreases from -3.7‰ at 210 maOD to -7.3‰ at 613 maOD. Uncorrected $\delta^{18}O$ in quartz shows an opposite trend, with $\delta^{18}O$ increasing from $+13.9$ to $+15.1\text{‰}$ over the same elevation interval.

4.2 Hydrogen isotopes

Hydrogen isotope data for extracted inclusion fluids along with summary fluid inclusion and assay–elevation data are also presented in Table 1. δD varies between -68.0 and -19.0‰ . As with the oxygen data, with the exception of three samples, δD shows a strong correlation with sample–elevation varying from the lightest values (-47.8‰) at highest elevations (613 maOD) to the heaviest (-19‰) at the lowest (210 maOD).

Combined δD and $\delta^{18}O$ data are presented in Figure 2, and where both δD and $\delta^{18}O$ were measured on the inclusion fluids, they show a clear trend that is sub-linear and parallels the Mediterranean Meteoric Water Line (MMWL). No fractionation correction has been applied to the $\delta^{18}O$ fluid inclusion water data. Moreover, the data bear a striking similarity to those for the modern geothermal system.

Two liquid–vapour (boiling) fractionation trends are also shown with a corresponding reservoir composition. The fractionation trends are calculated for single-stage steam-separation, with the points showing end-member equilibrium compositions of liquid and vapour. Fluid inclusions trapping mixtures of these two end members (heterogeneous trapping) will have isotopic compositions that fall along the tie-lines, though the position of fractionation lines in δD — $\delta^{18}O$ space is dependent on the initial choice of reservoir composition. It is clear that where both isotope ratios were determined on the inclusion fluids the data are well explained by boiling and heterogeneous trapping, which agrees with the fluid inclusion microthermometry (see Fig. 1).

In addition to the uncorrected fluid inclusion and geothermal water data, estimated hydrothermal fluid compositions are also illustrated in Figure 2. These were calculated using quartz–water fractionation factors and mean fluid inclusion temperatures. Here the data show considerable scatter and are difficult

Table 1. Stable isotope data for Profitis Ilias inclusion fluids and quartz. Also shown are summary microthermometric data, gold-silver concentrations and boiling curve temperatures for each sample elevation

Sample no.	Elevation (maOD)	Sample wt. (g)	FI water weight (mg)	$\delta^{18}\text{O}\%$ quartz	$\delta^{18}\text{O}\%$ FI water	$\delta\text{D}\%$ FI water	Au (ppm)	Ag (ppm)	Salinity (wt % NaCl eq.)	Th range ($^{\circ}\text{C}$)	boiling curve T ($^{\circ}\text{C}$)
G2185	657	1.4	0.5	15.4	-4.5	-28.7	7.18	20	6.1 -- 6.8	150 -- 160	89
G1746	621	0.5	2.5	15.5	-7.8	-51.0	56.50	62	5.0 -- 5.5	213 -- 243	149
G1810	613	0.5	0.3	15.1	-7.3	-47.8	n.d.	n.d.	4.5 -- 4.5	161 -- 284	156
G2374	551	1.5	1.2	14.2	-7.8	-68.0	4.22	10	3.4 -- 5.6	190 -- 234	188
G2245	499	0.5	3.7	14.6	-6.9	-41.5	18.00	13	3.3 -- 4.9	205 -- 215	204
G2255	457	0.5	1.6	13.9	-6.1	-39.8	4.84	15	3.1 -- 4.7	190 -- 219	213
G2424	421	0.7	1.2	14.2	-6.2	-50.5	6.32	17	0.0 -- 7.5	233 -- 253	220
G2267	405	1.4	3.7	14.3	-4.1	-33.3	8.51	3	6.5 -- 7.8	223 -- 249	223
G2268	403	1.2	2.5	13.7	-4.5	-34.9	10.20	11	4.4 -- 9.2	208 -- 231	223
G2283	365	1.2	0.3	13.4	-3.7	-23.8	10.20	11	3.1 -- 6.2	219 -- 251	230
PD9380	210	0.5	1.2	13.9	-3.7	-19.0	n.d.	n.d.	5.6 -- 5.6	249 -- 249	250

to relate to steam fractionation and the modern geothermal system.

5 CONCLUSIONS

Boiling appears to exert a major control on the location of ore. This is seen in both the microthermometric and the "fluid" stable isotope data.

The inclusion–fluid stable isotope data can be readily compared to the modern geothermal system, whereas the relationship between the fluid–mineral data and those of the modern system is more ambiguous

We suggest that data derived by analysing both δD and $\delta^{18}\text{O}$ on inclusion fluids can provide a better framework for interpreting fluid processes in epithermal systems than current methodologies based on calculating $\delta^{18}\text{O}$ from fluid–quartz equilibria.

6 ACKNOWLEDGEMENTS

Midas SA is thanked for allowing access to proprietary geological information, drill–core and assay records. The research was supported by the Joint Research Programme for Economic Geology between the Greek Secretariat General for Research and the British Council. Permission to publish for JN, MJL, TJS and BS is by the Director, British Geological Survey, NERC.

7 REFERENCES

Christianis K., & St. Seymour K. 1995. A study of scale deposition: an analogue of meso- to epithermal ore formation in the volcano of Milos, Aegean Arc, Greece. *Geothermics* 24: 541 - 552.

Kilias, S., Naden, J., Cheliotis, I., Shepherd, T.J., Constandinidou, H., Crossing, J. & Simos, I. *in press*. Epithermal gold mineralisation in the active Aegean Volcanic arc: the Profitis Ilias deposit, Milos island, Greece. *Mineralium Deposita*.

Lécuyer, C. & O'Neil, J.R. 1994. Stable isotope compositions of fluid inclusions in biogenic carbonates. *Geochim. Cosmochim. Acta* 58: 353-363.

Liakopoulos A., Katerinopoulos A., Markopoulos T. & Boulegue, J. 1991. A mineralogical, petrographic and geochemical study of samples from wells in the geothermal field of Milos Island (Greece) *Geothermics* 20: 237–256.

Ligang, Z., Jingxiu, L., Huanbo, Z. & Zhensheng, C. 1989. Oxygen isotope fractionation in the quartz-water-salt system. *Econ. Geol.* 84: 1643 - 1650

Ohba, T., Kazahaya, K. & Matsuo, S. 1995. Diffusional ^{18}O loss from inclusion water in a natural hydrothermal quartz from the Kaneuchi tungsten deposit, Japan. *Geochim Cosmochim Acta* 59: 3039 – 3047.

Ohba, T. & Matsuo, S. 1988. Precise determination of hydrogen and oxygen isotope ratios of water in fluid inclusions of quartz and halite. *Geochemical Journal*, 22: 55 – 68.

Pflumio, C., Boulegue, J., Liakopoulos, A. & Briquieu, L. 1991. Oxygen, hydrogen, strontium isotopes and metals in the present-day and past geothermal systems of Milos island (Aegean arc). In: Pagel and Leroy (eds.): *Source, transport and deposition of metals*. Balkema, Rotterdam.

Vytik, M.O., Krouse, H.R. & Demihov, Y.N. 1993. Preservation of $\delta^{18}\text{O}$ values of fluid inclusion water over geological time in an epithermal environment: Beregovo deposit, Transcarpathia, Ukraine. *Earth and Plan. Sci. Lett.* 119: 561 – 568.